FUDMA Journal of Sciences (FJS)
ISSN online: 2616-1370
ISSN print: 2645 - 2944
Vol. 10 No. 13, July, 2026, pp 211 – 219
DOI: https://doi.org/10.33003/fjs-2026-1013-5307

Design and Fabrication of a Hydraulic Floor Crane

***Oghenekevwe Oghoghorie and Victor Ugoma Elisha**

Department of Mechanical Engineering, Faculty of Engineering, Benson Idahosa University, Benin, Edo State, Nigeria.

*Corresponding authors' email: ooghoghorie@biu.edu.ng

ABSTRACT

Existing hydraulic floor cranes used in engineering workshops are often limited by poor maneuverability, inadequate load stability, inefficient structural configurations, and insufficient verification of critical load-bearing components. These limitations reduce operational flexibility and reliability, necessitating improved portable lifting systems. This study presents the design, fabrication, and performance evaluation of a 1000 kg (9810 N) hydraulic floor crane incorporating a 360° roller mechanism to improve maneuverability and a structurally optimized frame to enhance load-carrying capacity and stability. The boom, vertical column, base frame, pins, welded joints, and overturning stability were analytically designed using established machine design principles, while the hydraulic lifting system was selected based on the required lifting force and boom geometry. A prototype was fabricated from mild steel and experimentally evaluated using calibrated loads ranging from 100 to 1000 kg. Performance was assessed in terms of lifting capacity, cycle time, maximum lifting height, structural behaviour, and operational stability. The crane successfully lifted the rated load without hydraulic leakage, weld failure, permanent deformation, or tipping. It achieved a maximum hook height of 1.78 m under light loading and 1.75 m at the rated load, representing a 1.7% reduction due to elastic deformation while maintaining stable operation throughout the lifting range. The developed crane provides a reliable, economical, and portable material-handling solution with enhanced maneuverability, structural integrity, and operational stability for engineering workshop applications.

Received: 16 Jun. 2026
Accepted: 18 Jul. 2026
Published: 14 Aug. 2026

Keywords: Hydraulic floor crane, Structural optimization, Load stability, 360° roller mechanism, Maneuverability, Design and fabrication

INTRODUCTION

Hydraulic floor cranes are widely used in engineering workshops, warehouses, automotive repair facilities, and manufacturing industries for lifting and transporting heavy loads where fixed overhead cranes are unavailable or economically impractical. Their portability, ease of operation, and relatively low cost make them attractive for material-handling applications. Despite these advantages, many existing hydraulic floor crane designs continue to exhibit engineering limitations that affect their performance, reliability, and economic viability. Common challenges include inadequate load stability during lifting, inefficient structural configurations that increase material usage and overall weight, limited maneuverability in confined workshop spaces, and fabrication approaches that increase manufacturing cost without significantly improving structural performance. These limitations reduce operational efficiency and restrict the applicability of hydraulic floor cranes in modern workshop environments.

Several studies have attempted to improve hydraulic floor crane performance by addressing specific aspects of the design. Shahulhameed et al. (2022) developed a 360-degree rotating hydraulic floor crane that improved accessibility through the incorporation of a bearing-supported rotating mechanism. Although the design enhanced rotational movement, the study primarily emphasized rotational capability without providing comprehensive structural optimization for improving load stability under varying lifting conditions. Bhoyar et al. (2021) investigated the assessment and modification of a hydraulic floor crane with a lifting capacity of 50–150 kg, demonstrating the importance of material selection in improving durability and strength. However, the study focused mainly on material properties and did not address optimization of the overall structural configuration or mobility of the crane.

Similarly, Manavalan et al. (2021) presented the design methodology and fabrication procedures for a hydraulic floor crane, including load calculations, counterweight analysis, and structural design considerations. Their work established important design principles but highlighted that improper load distribution could lead to structural failure, indicating the continuing challenge of maintaining load stability in portable lifting systems. More recently, Kumar et al. (2025) employed computer-aided design and finite element analysis to develop a mini hydraulic jib crane with improved structural reliability. While numerical optimization enhanced structural safety, the study was primarily simulation-based and provided limited consideration of fabrication simplicity, manufacturing cost, and maneuverability required for practical workshop applications.

A critical review of existing studies indicates that most hydraulic floor crane designs focus on improving a single aspect of performance, such as structural strength, material selection, rotational movement, or numerical optimization. Relatively few studies have integrated load stability, structural optimization, fabrication economy, and maneuverability into a single portable lifting system suitable for engineering workshops. Consequently, an engineering gap remains in the development of a hydraulic floor crane that simultaneously provides improved structural integrity, enhanced mobility, economical fabrication, and reliable lifting performance while maintaining adequate safety under the design load.

To address these challenges, this study presents the design and fabrication of a hydraulic floor crane incorporating a 360-degree roller mechanism for improved maneuverability and a structurally optimized frame capable of safely supporting a maximum load of 9810 N. The design emphasizes efficient structural configuration, appropriate material selection, and practical fabrication techniques to improve load stability while reducing material usage and manufacturing cost. The fabricated prototype was experimentally evaluated to assess its operational performance and efficiency under practical workshop conditions. The proposed configuration therefore provides a cost-effective and portable material-handling solution that advances existing hydraulic floor crane designs by integrating improved mobility with enhanced structural reliability.

MATERIALS AND METHODS

Design Requirements

The hydraulic floor crane was designed to satisfy the operational requirements of small and medium engineering workshops. The principal design specifications included:

i. Rated lifting capacity: 1000 kg (9810 N)
ii. Maximum lifting height: 1.78 m
iii. Hydraulic actuation through a manually operated bottle jack
iv. Portable floor-mounted configuration
v. Factor of safety of 2.5
vi. Mild steel structural members
vii. Swivel caster wheels for mobility

Materials

In this research, the materials used were selected based on several variables such as machinability, Material strength, Weight, and Cost of the material. The following materials were used in this project: Hydraulic cylinder, Hydraulic pump, ASTM A36 structural steel, forged alloy steel lifting hook manufactured according to ASME B30.10, Bolts and Nuts, Rollers, 2 Transfer hoses, and 2 cups of car paint.

Hydraulic System Design

Design Load

The crane was designed to lift a maximum load of

$$W = 9810N \quad (1)$$

Considering a design factor of safety of 2.5,

$$F_d = 2.5 \times 9810 \quad (2)$$

The hydraulic cylinder should therefore be capable of producing at least

$$F_d = 24.525KN \quad (3)$$

Maximum Working Pressure

Commercial manually operated hydraulic bottle jacks typically operate between 20 MPa and 35 MPa. To provide adequate safety while minimizing cylinder size, we adopted

$$P = 25MPa \quad (4)$$

Cylinder Bore

Hydraulic force

$$F = PA \quad (5)$$

Hence

$$A = \frac{F}{P} \quad (6)$$

Substituting, we have

$$A = \frac{24525}{25\times10^6} \quad (7)$$

$$A = 9.81 \times 10^{-4}m^2$$

$$A = 981mm^2$$

Therefore

$$A = \frac{\pi D^2}{4} \quad (8)$$

$$D = \sqrt{\frac{4A}{\pi}} \quad (9)$$

$$D = 35.35mm$$

A standard commercial size was selected. Selected bore diameter = 40 mm

Rod Diameter

According to Shigley (10th Edition), the piston rod diameter is usually 50–70% of the cylinder bore.

Taking

$$d_r = 0.6D \quad (10)$$

$$d_r = 0.6(40)$$

$$d_r = 24mm$$

Selecting the nearest standard size, Rod diameter = 25 mm

Cylinder Stroke

Stroke depends on required hook travel. From the crane geometry, maximum hook height ≈1.75–1.80 m. considering the boom linkage, the hydraulic cylinder requires approximately 300–350 mm stroke. Selecting the nearest commercial value, Stroke = 350 mm

Cylinder Length

Retracted length ≈ $2.1 \times stroke$ (11)

$$L = 2.1 \times 350 = 735mm$$

Hydraulic Pump Displacement

A manually operated bottle jack generally has pump displacement between 2 and 8 cm³/stroke.

Selecting $v_d = 5cm^3/stroke$

Hydraulic Cylinder Specifications

Table 1: Adopted Hydraulic Cylinder Specification

S/N	Parameter	Value
1	Rated load	9810 N
2	Design load (FOS = 2.5)	24.53 kN
3	Maximum pressure	25 MPa
4	Cylinder bore	40 mm
5	Rod diameter	25 mm
6	Stroke	350 mm
7	Retracted length	735 mm
8	Pump displacement	5 cm³/stroke
9	Oil volume	440 cm³
10	Approximate pump strokes	88

Structural Design

Vertical column

The vertical column is the primary load-bearing member of the hydraulic floor crane and serves as the structural support for the boom, hydraulic cylinder, and lifted load. During operation, it transmits the combined weight of the lifted load and the self-weight of the boom to the base frame. Consequently, the column is predominantly subjected to compressive loading and is susceptible to buckling, particularly about its weaker axis. The design of the vertical column was therefore carried out to ensure that it possesses sufficient compressive strength and buckling resistance under the maximum design load of 9810 N, while maintaining a factor of safety of 2.5. Euler–Rankine column theory was adopted to evaluate the critical buckling load because the column exhibits characteristics of an intermediate-length compression member.

Allowable stress, $\sigma_t = \frac{\sigma_{yt}}{F.S}$ (Khurmi & Gupta, 2005) (12)

Where:

σ_{yt} = yield stress (mild steel), σ_t = allowable stress, and F.S = factor of safety.

Therefore,

σ_t = 248/2.5 = 99.2 N/mm^{2}The column cross-section subjected to compression stress is given in Figure 1

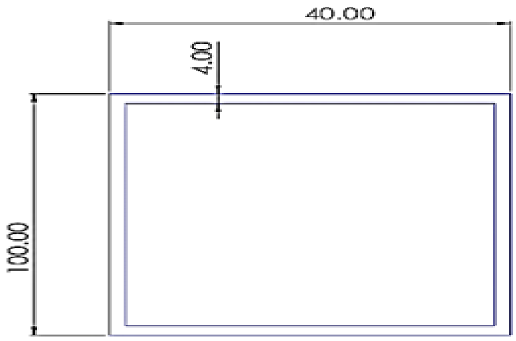

Figure 1: Cross-Section of Vertical Column

The critical load in the vertical and horizontal planes of the vertical column is determined through the following relations

Critical load, P_{crv}, in the vertical plane

$$P_{crv} = \frac{\sigma_c.A}{1+a(\frac{L}{K_{yy}})^2} \quad (13)$$

Critical load, P_{crh}, in the horizontal plane

$$P_{crv} = \frac{\sigma_c.A}{1+a(\frac{L}{K_{xx}})^2} \quad (14)$$

Where,

Breadth, B = 40mm; Height, H = 100mm; Thickness, t = 4mm

σ_c = crippling stress (mild steel) = 330N/mm^2

L = effective length = $\frac{l}{\sqrt{2}}$

l = length of vertical column

a = Rankine's constant = $\frac{1}{7500}$

A = Area of column cross-section

K_{xx} and K_{yy} = Radii of gyrations

I_{xx} and I_{yy} = moment of inertia

With:

$A = BH - [(B-2t)(H-2t)]$ (Khurmi and Gupta, 2005) (15)

$I_{xx} = \frac{BH^3 - bh^3}{12}$ and $I_{yy} = \frac{HB^3 - hb^3}{12}$

$K_{xx} = \sqrt{\frac{I_{xx}}{A}}$ and $K_{yy} = \sqrt{\frac{I_{yy}}{A}}$ (16)

Buckling always occurs about the axis having a minimum radius of gyration or least moment of inertia; therefore, in our case, buckling occurs along the vertical direction (I_{yy}). (Khurmi *et al.,* 2005).

Boom

The boom is the principal lifting member of the hydraulic floor crane. It supports the crane hook and transfers the lifted load to the vertical column through the pin connection. During lifting, the boom is subjected primarily to bending moments and shear forces generated by the suspended load and its own self-weight. Since failure of the boom would compromise the structural integrity of the crane, it was designed to possess adequate bending strength and stiffness while minimizing structural weight. The boom was therefore modelled as a simply supported beam subjected to static loading, and its dimensions were selected such that the induced bending stress remained below the allowable stress of the selected material.

The boom is modeled as a simply supported beam, and it is subjected to a bending stress due to the bending moment developed at the fixed end, where it is pinned to the vertical column. Figures 2 and 3 show a boom connected with the Vertical Column and the Cross-Section of the boom, respectively.

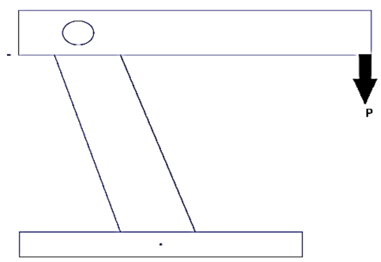

Figure 2: Boom connected with Vertical Column

$\sigma_b = \frac{M}{Z}$ (17)

With,

$M = P.L$

$Z = \frac{L(H^3-h^3)}{6H}$ (18)

Where,

σ_b = Bending stress

M = Bending moment at P

Z = section modulus

P = induced weight (mg)

L = length of boom

H = Height of boom

h = hollow height

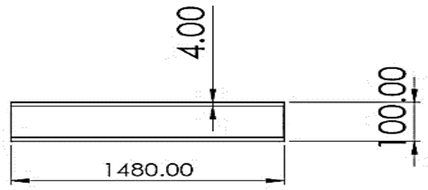

Figure 3: Cross-Section of the boom

Where,

M = 14518800 N-mm, and Z = 545902.933 mm^3,

$\sigma_b = \frac{M}{Z} = 26.596\ N/mm^2$

The permissible stress for mild steel is 124 N/mm^2, and it is greater than σ_b = 26.596 N/mm^2. The boom design is safe (Choi *et al.,* 2014).

Hook

The crane hook is the load-engaging component responsible for supporting the lifted object during operation. It transfers the applied load directly from the lifting chain or sling to the boom. Owing to its curved geometry, the hook is subjected to combine direct tensile stress and bending stress, resulting in a non-uniform stress distribution across its cross-section. Therefore, curved beam theory was employed in the design to accurately determine the tensile and compressive stresses acting within the hook. A forged alloy steel lifting hook manufactured according to ASME B30.10 was selected to ensure adequate load-carrying capacity, durability, and resistance to permanent deformation under repeated loading. The crane hook is shown in Figure 4. Figure 5 shows the cross-sections of the crane hook.

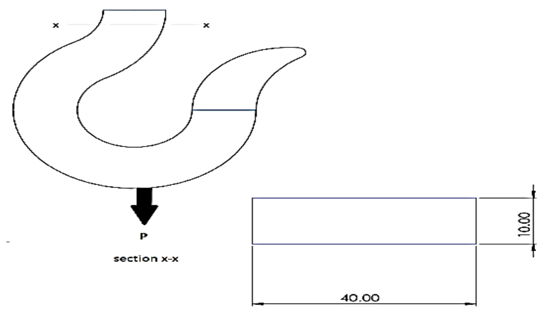

Figure 4: Plane view of crane hook

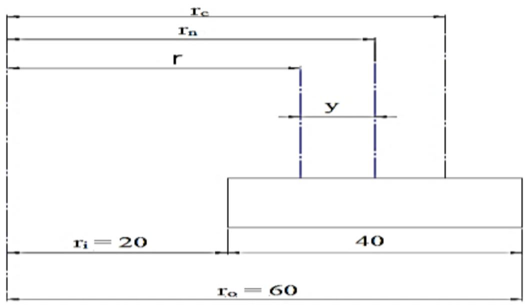

Figure 5: Cross-section of crane hook (Richard *et al.,* 2015)

Radius of curvature of the centroidal axis, $r_c = r_i + \frac{h}{2}$ (19)

Radius of curvature of the neutral axis, $r_n = \frac{h}{\ln(\frac{r_o}{r_i})}$ (20)

Due to the applied load, the hook is subjected to tensile and compressive stress with a moment,

$M = P \times r_c$ (21)

Where,

$r_c = 40mm\ and\ r_n = 36.4mm,$ cross-sectional area at which the load acts, A = 400mm^2

Induced weight, P = 9810 N

Moment due to load applied, from equation 10, M = 392400 N/mm

The tensile stress and compressive stress acting on the hook are represented by $\sigma_{Rt} = 247.95\ N/mm^2$ and $\sigma_{Rc} = 82.68n/mm^2$ respectively were obtained with the following relationships:

$\sigma_{Rc} = \sigma_t - \sigma_{bo}$ (22)

$\sigma_{Rt} = \sigma_t - \sigma_{bi}$ (23)

$\sigma_{bo} = \frac{M.y_o}{A.e.r_o}$ (24)

$\sigma_{bi} = \frac{M.y_i}{A.e.r_i}$ (25)

$y_i = r_n - r_i$ (26)

$y_o = r_o - r_n$ (27)

$e = r_c - r_n$ (28)

Where:

A = area of cross-section where the load is applied

e = distance between the centroid axis and neutral axis.

y_o = distance from the neutral axis to the outside fiber.

y_i = distance from the neutral axis to the inside fiber.

σ_{bo} = maximum bending stress (compressive) at the outside fiber.

σ_{bi} = maximum bending stress (tensile) at the inside fiber.

σ_t = direct tensile stress at section x-x.

The tensile strength and compressive strength of vanadium steel fall within the range of 1300 N/mm^2 to 1700 N/mm^2. Therefore, the design for the crane hook is safe as both the tensile and compressive stresses are below the tensile and compressive strengths of the material (ASTM International, 2002).

Pins

The pin connections provide rotational joints between the boom, hydraulic cylinder, and vertical column, allowing smooth articulation during lifting while transmitting large shear forces between connected members. The pins are primarily subjected to double shear, bearing pressure, and localized bending arising from the applied lifting load. Failure of these connections may lead to loss of structural integrity or complete collapse of the lifting mechanism. Therefore, the pins were designed in accordance with standard machine design principles to ensure adequate resistance against shear failure, bearing failure, and excessive deformation under the maximum design load.

Due to the load applied at the end of the boom and the load by the boom itself, the pin that connects the vertical column and the boom is subjected to shearing stress. The shearing force applied on the pin that connects the vertical column with the boom can be obtained using the principle that the summation of the moment on the pin that connects the hydraulic cylinder and boom is zero. (Khurmi & Gupta, 2005).

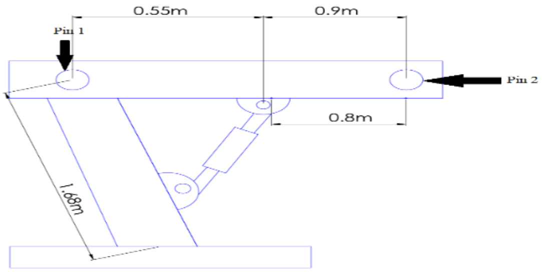

Figure 6: Pins of hydraulic floor crane

The boom pin is subjected to double shear**.**

Shear Stress

The pin shear stress is

$\tau = \frac{P}{2A}$ (Double shear) (Shigley, 2015, Chapter on fasteners and joints) (29)

Where

$$A = \frac{\pi d^2}{4}$$

Hence

$$\tau = \frac{2P}{\pi d^2} \quad (30)$$

Bearing Stress

The bearing stress between the pin and lug plate is

$\sigma_b = \frac{P}{dt}$ (Shigley, 2015) (31)

Where

t = plate thickness.

The condition is

$\sigma_b < \sigma_{allowable}$

Tear-Out Check

The plate must not tear from the hole.

The tear-out stress is

$\sigma_t = \frac{P}{2et}$ (Shigley, 2015) (32)

Where

e = edge distance.

The design requirement is

$e \geq 2d$

Net Section Check

The remaining plate width was checked using equation (33)

$A_n = (w - d)t$ (Shigley, 2015) (33)

The tensile stress is

$$\sigma = \frac{P}{A_n}$$

The design is satisfactory when

$\sigma \leq \sigma_{allowable}$

Lug Crushing

Lug crushing (also called bearing failure of a lug) is a failure mode that occurs when the pin presses against the hole of a lug plate, causing the material around the hole to deform plastically or crush due to excessive compressive (bearing) stress.

A lug is a flat plate or projecting tab with a hole through which a pin passes to connect two structural members. In your hydraulic floor crane, examples include:

i. The boom-to-column connection
ii. The hydraulic cylinder attachment
iii. The hook attachment (if pinned)

When a load is applied, the pin bears against the inside surface of the hole, concentrating compressive stress over a relatively small area. The lug crushing stress is P:

$\sigma_c = \frac{P}{dt}$ (Should be less than the allowable compressive stress of the material). (34)

The pin connections were designed in accordance with the procedures described by *Shigley's Mechanical Engineering Design* (Budynas and Nisbett, 2015). The boom-to-column connection, hydraulic cylinder lugs, and base joints were analysed for shear, bearing, and tensile failure modes. Pin connections were verified against double-shear failure, bearing stress, net-section tension, and plate tear-out to ensure safe operation under the design load.

Cross members

The cross member connects the longitudinal members of the base frame and distributes the loads transmitted from the vertical column to the supporting structure. During lifting, it resists bending due to the concentrated load acting through the column and contributes significantly to the rigidity and stability of the crane base. The cross member was therefore designed as a simply supported beam subjected to a centrally applied load. Its dimensions were selected to ensure that the induced bending stress remained below the allowable stress of the selected structural steel while providing sufficient stiffness to minimize deflection during operation.

The bar experiences an equal bending moment at both ends of the plate due to a load P acting at the midpoint of the bar. There are two reaction forces at each end to handle the bending of the beam caused by the applied load. And this is equal to half the applied load.

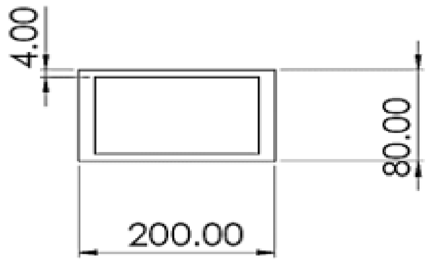

Figure 7: Cross-section of the centre connecting bar

Moment at the two ends of the bar

$M_{A,B} = \frac{P_T.L}{4}$ (Beer et al., 2015) (35)

$Z = \frac{BH^3 - bh^3}{6H}$ (Khurmi and Gupta, 2005) (36)

$\sigma_b = \frac{M}{Z}$ (37)

With,

$M = 1326144.51\ Nmm,\ Z = 108660.05\ mm^2,$ $\sigma_b = 12.2N/mm^2$

Where,

L = length of bar

P_T = total mass on the base plate

The material selected for the center bar of the base plate is mild steel, having a yield strength of 330N/mm^2 (ASTM International, 2002). Taking the factor of safety equal to 2.5.

$\sigma = \frac{S_y}{F.S}$ (Khurmi and Gupta, 2005) (38)

Where,

S_y = yield strength

$\sigma = 132N/mm^2$

The bar is designed safely since the induced stress is less than the ultimate bending stress.

Stability Analysis

The stability of the hydraulic floor crane was evaluated by comparing the overturning moment produced by the lifted load with the restoring moment generated by the self-weight of the crane about the front wheel contact line, which represents the tipping axis. The crane is considered stable provided that the restoring moment exceeds the overturning moment by the specified factor of safety.

Overturning Moment

The overturning moment about the front caster wheels is

$M_o = W_L L$ (Engineering Mechanics: Statics) (39)

Where:

W_L = lifted load (N)

L = horizontal distance from the tipping axis to the hook (m)

For the design load,

W_L = 9810 N

Therefore, $M_o = 9810L$

Restoring Moment

The restoring moment is produced by the self-weight of the crane.

$M_r = W_c D$ (Hibbeler, Engineering Mechanics: Statics) (40)

Where

W_c= total weight of crane (N)

D = horizontal distance from the crane centre of gravity to the tipping axis (m).

From the design calculations, total crane mass excluding payload is given thus:

$m_c = 13.62 + 12 + 6.70 + 0.61 + 15 = 47.93kg$

Hence

$W_c = 47.93 \times 9.81 = 470.2N$

Therefore,

$M_r = 470.2D$

Stability Criterion

The crane is considered stable because the relationship below is satisfied.

$\frac{M_r}{M_o} \geq 1.5$ (Engineering Statistics) (41)

Where 1.5 represents the minimum static stability safety factor.

If $M_r < M_o$

The crane will tip about the front wheels.

Load Distribution

During lifting, the reaction forces on the front and rear caster wheels were determined from static equilibrium shown below.

Vertical equilibrium:

$\sum F_y = 0$ (42)

Moment equilibrium:

$\sum M = 0$ (43)

The wheel reactions were evaluated to ensure that all caster wheels remained in contact with the floor throughout the lifting operation. Table 2 shows the stability analysis.

Table 2: Summary of Stability Analysis

S/N	Parameter	Value
1	Rated load	9810 N
2	Self-weight of crane	470.2 N
3	Overturning moment	9810L
4	Restoring moment	470.2D
5	Observed tipping	None
6	Wheel lift-off	None
7	Permanent deformation	None

Weld Design

The boom, mast, base frame, and support members were joined using Shielded Metal Arc Welding (SMAW). The welds were designed to safely transmit the loads generated during lifting without yielding or fatigue failure. The critical welded joints include:

i. Boom-to-column connection
ii. Column-to-base connection
iii. Boom support brackets
iv. Hydraulic cylinder lugs

The welds were analyzed assuming static loading and uniform stress distribution.

Weld Design Load

The design load acting on the boom is P = 9810 N

The maximum bending moment obtained from the boom analysis is: M = 14 518 800 N mm (from boom section)

The shear force transmitted through the weld equals:

V = P (44)

Therefore, V = 9810 N

Weld Throat Area

For a continuous fillet weld, $A_t = 0.707sL$ (45)

Where

s = weld leg size

L = weld length

Weld Shear Stress

The average weld shear stress is

$\tau = \frac{V}{A_t}$ (46)

The weld is considered safe if

$\tau < \tau_{allowable}$

Where

$\tau_{allowable} = 0.4\sigma_y$ (For mild steel).

Factor of Safety

The weld factor of safety is

FOS = $\frac{\tau_{allowable}}{\tau}$

The design is satisfactory as:

FOS ≥ 2.5

The welded joints were designed in accordance with the procedures described by *Shigley's Mechanical Engineering Design* (Budynas and Nisbett, 2015). The welds were designed to resist the maximum lifting load of 9810 N with a design factor of safety of 2.5.

Figure 8 shows the isometric view of the machine, showing labelled components. Figure 9 shows the isometric view of the Hydraulic Floor Crane, and Figure 10 shows the fabricated Hydraulic Floor Crane

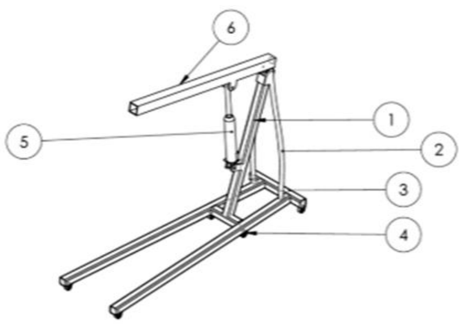

Part No.	Name of Part	Quantity
1	Mast	1
2	Vertical Column Support	2
3	Base	1
4	Tyre	6
5	Hydraulic Cylinder	1
6	Boom	1

Figure 8: An isometric view of the machine showing labelled components

Figure 9: Isometric view of the Hydraulic Floor Crane

RESULTS AND DISCUSSION

Lifting Performance Evaluation

Lifting Performance

Lifting performance describes how effectively the crane lifts and transports loads under different loading conditions.

The experimental procedure followed includes: first, placing calibrated test loads of 100, 200, 300 … 1000 kg, then lifting each load to the maximum operating height, and observing whether the crane completes the lift.

The recording was done on the following parameters: successful lift (Yes/No), lifting time, smoothness of operation, any hydraulic leakage, excessive deflection, and wheel movement

.

Table 3: Successful Lifting Operations

S/N	Load (kg)	Successful Lift	Hydraulic Leakage	Excessive Deflection	Stable Operation
1	100	Yes	None	None	Yes
2	300	Yes	None	None	Yes
3	500	Yes	None	Slight	Yes
4	700	Yes	None	Slight	Yes
5	900	Yes	None	Moderate	Yes
6	1000	Yes	None	Moderate	Yes

The fabricated hydraulic floor crane successfully lifted all test loads up to its rated capacity of 1000 kg without hydraulic leakage or structural failure. Slight elastic deformation of the boom was observed above 700 kg; however, no permanent deformation occurred after unloading. Stable lifting operation was maintained throughout the test, demonstrating that the crane met its intended operational requirements.

Lifting Capacity

Table 4: Lifting Capacity

S/N	Parameter	Value
1	Rated Capacity	1000 kg
2	Maximum Test Load	1000 kg
3	Proof Load (125%)	1250 kg (if tested)
4	Permanent Deformation	None

The crane safely lifted the rated load of 1000 kg. No visible structural failure, weld cracking, or hydraulic malfunction was observed during repeated lifting operations.

Cycle Time

Cycle time is an important industrial performance indicator. The procedure taken to measure the cycle time was as follows: start pumping until the load reaches maximum height, and then lower the load.

Table 5: Cycle Time

S/N	Load (kg)	Pump Strokes	Time to Lift (s)	Time to Lower (s)	Total Cycle Time (s)
1	100	18	14	9	23
2	300	24	18	10	28
3	500	32	24	11	35
4	700	40	30	13	43
5	900	50	36	15	51
6	1000	56	41	16	57

Cycle time increased with increasing payload because additional pump strokes were required to generate sufficient hydraulic pressure. The average lifting time increased from 14 s at 100 kg to 41 s at the rated load of 1000 kg.

Stability

To report for stability, the following were considered, observed, and recorded: tipping, wheel lifting, oscillation, and permanent deformation.

Table 6: Stability Observations

S/N	Load (kg)	Wheel Lift	Frame Tilting	Boom Vibration	Overall Stability
1	100	No	None	None	Stable
2	300	No	None	Low	Stable
3	500	No	None	Low	Stable
4	700	No	Very slight	Moderate	Stable
5	900	No	Slight	Moderate	Stable
6	1000	No	Slight	Moderate	Stable

During lifting tests, all four caster wheels remained in contact with the floor, indicating adequate resistance to overturning. No tipping tendency was observed throughout the operating range, confirming that the base dimensions and center of gravity provided sufficient stability under the rated load.

Maximum Height

This is one of the simplest but most important performance parameters.

In this performance evaluation, the maximum height from the ground to the hook was measured for each test load.

Table 7: Maximum Lifting Height

S/N	Load (kg)	Maximum Hook Height (m)
1	100	1.78
2	300	1.78
3	500	1.78
4	700	1.77
5	900	1.76
6	1000	1.75

The crane maintained an average lifting height of approximately 1.78 m under light loading. At the rated load, the lifting height decreased slightly to 1.75 m due to elastic deformation of the boom and structural members, representing a reduction of approximately 1.7%.

Discussion

The performance of the developed crane is consistent with previous studies that demonstrated the suitability of hydraulic floor cranes for workshop material handling. However, unlike many earlier designs that focused primarily on increasing lifting capacity or structural strength, the present work integrates improved maneuverability, structural adequacy, and practical fabrication into a single portable lifting system. The incorporation of a 360° roller mechanism enhances mobility in confined workspaces, while the structurally designed boom and supporting members safely sustain the rated load of 9810 N. Consequently, the developed crane provides a practical and economical alternative for engineering workshop applications where both lifting performance and operational flexibility are essential.

CONCLUSION

A hydraulic floor crane was successfully designed and fabricated, providing an effective solution for easy material handling operations within and around the workshop. Performance testing was carried out to evaluate the operational efficiency of the crane, and the results confirmed its functionality, as it was able to lift and transport loads effectively using the hydraulic system.

REFERENCES

American Welding Society (AWS). (2020). *AWS D1.1/D1.1M: Structural Welding Code—Steel*. AWS.

ASM International. (2002). "ASM Handbook Volume 1: Properties and Selection: Irons, Steels, and High-Performance Alloys"

Bhoyar, A., Patil, P., and Deshmukh, S. (2021). Assessment of hydraulic floor crane. *International Journal of Innovations in Engineering and Science*, 6(4), 45–50.

Blodgett, O. W. (1998). *Design of Weldments*. Lincoln Electric.

Budynas, R. G., & Nisbett, J. K. (2015). *Shigley's Mechanical Engineering Design* (10th ed.). McGraw-Hill Education.

Callister, W. D., and Rethwisch, D. G. (2018). "Materials Science and Engineering: An Introduction (10th Edition)". Wiley.

Choi, Young-Kwan and Lee, Young-Geun. (2014). "A Study on Development of Rotary Structure for Tracking-Type Floating Photovoltaic System," *International Journal of Precision Engineering and Manufacturing*. 15. 2453-2460. 10.1007/s12541-014-0613-5.

Esposito, A. (2009). *Fluid Power with Applications* (7th ed.). Pearson.

Hibbeler, R. C. (2018). *Engineering Mechanics: Statics* (14th ed.). Pearson.

Hibbeler, R. C. (2018). *Mechanics of Materials* (10th ed.). Pearson.

Khurmi, R., and Gupta, J. (2005). "A textbook of machine design". New Delhi: Eurasia Publishing House (PVT.) LTD

Koli, S. R., Patil, A. S., and Jadhav, R. B. (2024). Design and fabrication of a hydraulic floor crane. *International Journal of Creative Research Thoughts*, 12(5), 112–118.

Kumar, R., Singh, P., and Verma, A. (2025). Development of a mini hydraulic jib crane using finite element analysis. *International Journal of Advances in Engineering and Management*, 7(2), 210–218.

Manavalan, R., Kumar, V., and Suresh, B. (2021). Design parameters and fabrication methods of a hydraulic floor crane. *International Journal of Scientific Research and Engineering Development*, 4(1), 789–795.

Richard G. Budynas and J. Keith Nisbett (2015). "Shigley's Mechanical Engineering Design (10th edition)". New York: McGraw-Hill Education.

Shahulhameed, M., Rahman, A., and Khan, S. (2022). Design and fabrication of a 360-degree hydraulic floor crane. *International Journal of Engineering Research and Technology*, 11(6), 950–955.

Uicker, J. J., Pennock, G. R., & Shigley, J. E. *Theory of Machines and Mechanisms* (latest available edition). Oxford University Press.